Proton NMR Investigations of the Smectic-C Phases of Three Alkyloxy-Azoxybenzenes

St. Limmer and M. Findeisen

Sektion Physik der Karl-Marx-Universität, Leipzig, GDR

Z. Naturforsch. **38 a**, 434–446 (1983); received October 4, 1982

Proton NMR investigations of the smectic-C phases of three 4,4′-bis-*n*-alkyloxy-azoxybenzenes (C_7, C_8, C_9) with temperature independent tilt angles are presented.

The behaviour of well-aligned samples (strong magnetic field $\gtrsim 1.5$ T, slow cooling rate) under rotation in the field can be described by the models of Luz and Meiboom, and Wise, Smith, and Doane, (LM/WSD), resp. However, on polarization of the samples in presence of magnetic fields $\lesssim 0.75$ T the molecular directors are not arranged preferentially parallel to the direction of the polarizing magnetic field but are rather inclined, i.e., the layers are stacked preferentially perpendicular to the original magnetic field direction (PSL model). It is shown that all the angular dependences of NMR second moments can be interpreted in terms of a superposition of the LM/WSD and PSL models, or, on the other hand, by assuming totally disordered fractions of the samples together with portions that fully obey the behaviour demanded by one of the above models (LM/WSD or PSL). The tilt angles derived from the comparison of experimental and theoretical angular dependences of the second moments for well-aligned samples are applied to the explanation of the experiments at lower polarizing fields successfully, too.

1. Introduction

In former investigations (see, e.g., [1, 2]) it has been shown and confirmed that the members of the homologous series of the 4,4′-bis-*n*-alkyloxy-azoxybenzenes exhibit a smectic-C phase beginning with the C_7 compound (Hept-OAB) which is not preceded by a smectic-A phase but appears directly on cooling down from the nematic phase. In Table 1 the transition temperatures of the first three compounds of this series having a smectic-C phase (Hept-, Oct-, Non-OAB corresponding to seven, eight, and nine carbon atoms in the alkyloxy chain, resp.) are listed.

The tilt angles remain constant throughout the whole smectic-C phase [1, 2]. Especially the smectic-C phase of Hept-OAB has been studied fairly thoroughly by different methods as, for example, X-ray [1–4], optical conoscopy [5], EPR [6, 7], NMR [8, 9], electric conductivity [10], with the aim of elucidating the structure and the dynamic molecular organisation of this phase. Although there is a general conformity in the explanation of the behavior of an oriented C phase under rotation in a sufficiently strong magnetic field the tilt angles derived at by different authors are covering a fairly wide range between about 30° and 45° (cf. Table 2).

Reprint requests to Dr. St. Limmer, Karl-Marx-Universität, Sektion Physik, DDR-7010 Leipzig, Linnestr. 5.

Table 1. Transition temperatures of the investigated compounds [11] (T_M-melting point, T_{CN}-smectic-C – nematic transition temperature, T_{NI} – clearing point, in °C).

Compound	T_M	T_{CN}	T_{NI}
Bis-heptyloxyazoxybenzene (Hept-OAB)	74.4	95.4	124.2
Bis-octyloxyazoxybenzene (Oct-OAB)	79.5	107.7	126.1
Bis-nonyloxyazoxybenzene (Non-OAB)	75.5	113.0	121.5

In most of the cases the experiments have been performed at only one polarizing field strength. As we shall outline below the experimental conditions (polarizing field strength, cooling rate) have a crucial influence on the quality of the overall orientation of the smectic-C sample. Only on very careful cooling down from the nematic phase and with polarizing fields above 1.5 T one (for these compounds) can reproducibly expect a homogeneously aligned sample with the long molecular axes being ordered (on the average) parallel to the magnetic field direction. Otherwise one has to take into account considerable deviations from the behaviour demanded by the model developed independently by Luz and Meiboom [8] and Wise, Smith, and Doane [9], which indeed could be proved by us experimentally (see Section 2).

0340-4811 / 83 / 0400-0434 $ 01.3 0/0. – Please order a reprint rather than making your own copy.

We try to give here a consistent description of not only one angular dependence but rather of a whole set of dependences for various polarizing field strengths.

For characteristic cases the angular dependences of the proton NMR lineshape have additionally been simulated corresponding to the different models and compared to the experimental ones.

2. Results

2.1. General expression for the second moment of the proton NMR lineshape in smectic-C phases

The basic prerequisites used in the calculation of the second moments are the same as in the former NMR investigations of smectic-C phases [8, 9]: It is demanded that the average direction of the long molecular axis ***d*** of a certain molecule is able to reorient nearly freely about the layer normal ***n*** (which is fixed for a given domain) so that ***d*** makes the minimum angle θ_H with the magnetic field ***B*** (minimum magnetic energy). Hence, the layer normal ***n***, the (average) long molecular axis ***d***, and the actual magnetic field direction ***B*** are co-planar.

Quite generally the second moment is defined as

$$M_2 = \frac{1}{N} \cdot \sum_{j=1}^{N} \sum_{k \neq (j)} \left(\frac{\overline{B_{jk}}}{2} \right)^2 , \tag{1}$$

where N is the number of protons, and

$$\overline{B_{jk}} = -\frac{3\gamma^2 \hbar}{r_{jk}^3} \left(\frac{3}{2} \overline{\cos^2 \vartheta_{jk}} - \frac{1}{2} \right) . \tag{2}$$

Here r_{jk} denotes the distance between protons j and k, γ the gyromagnetic ratio, and ϑ_{jk} the angle between the line connecting the protons j and k, and the magnetic field. The horizontal bar indicates averaging over all molecular orientations at a certain instant (or, equivalently, time averaging).

If we introduce a molecular frame of reference X, Y, Z (principal axes frame of the dipolar interaction between protons j and k; see also Figure 1), so that the Z-direction is defined by a certain inter-proton vector $\boldsymbol{r}_{jk}$ (e.g., the ortho benzene protons), i.e. appointing $\boldsymbol{e}_{jk} \equiv \boldsymbol{e}_Z$ ($\boldsymbol{e}_{jk}$ and $\boldsymbol{e}_z$ denote the corresponding unit vectors) one can rewrite the angular dependent term of (2) as follows:

$$\frac{3}{2} \overline{\cos^2 \vartheta_{jk}} - \frac{1}{2} = \frac{3}{2} \cdot (\boldsymbol{e}_H \boldsymbol{e}_Z)^2 - \frac{1}{2} \equiv S_{HH}^{ZZ} , \tag{3}$$

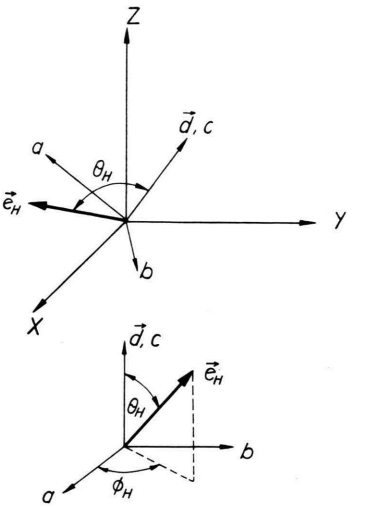

Fig. 1. Relative orientations of the frames of reference referred to in the text.

where S_{HH}^{ZZ} represents the order parameter of the Z-axis (≙ line connecting protons j and k) with respect to the direction of the magnetic field (characterized by unit vector $\boldsymbol{e}_H$). S_{HH}^{ZZ} can now be described in terms of three traceless tensors H_{kl}, $S_{kl}^{\alpha\beta}$, and $K_{\alpha\beta}^{ZZ}$ [12] by

$$S_{HH}^{ZZ} = \left(\frac{2}{3} \right)^2 \cdot H_{kl} \cdot S_{kl}^{\alpha\beta} \cdot K_{\alpha\beta}^{ZZ} . \tag{4}$$

Here H_{kl} denotes the field tensor which characterizes the direction of the magnetic field relative to an arbitrary laboratory frame (LF) x, y, z; $S_{kl}^{\alpha\beta}$ is the order tensor, and $K_{\alpha\beta}^{ZZ}$ describes the average molecular conformation. The indices α, β now specify the axes ξ, η, ζ, of a molecule-fixed frame (with ζ being parallel to the long molecular axis), and the indices k, l the axes x, y, z of the LF. Let a, b, c be the principal axes frame of the order tensor $S_{kl}^{\alpha\beta}$ in the LF. We choose the axis c so as to coincide approximately with the tilt direction (average direction of the long molecular axis within a domain), and a to lie in the plane of the smectic layer. b is perpendicular on both a and c (see also Figure 1). We shall sometimes refer to this as the "director frame". Then $S_{kl}^{\alpha\beta}$ characterizes the ordering of the molecular frame ($\alpha\,\beta = \xi, \eta, \zeta$) relative to the director frame ($k\,l = a, b, c$).

Neglecting transverse ordering (described by terms $S_{kl}^{\xi\xi} - S_{kl}^{\eta\eta}$) because of the relative smallness of

the corresponding order parameters [13, 14, 20] and therefore minor influence on the proton NMR data one can now express S_{HH}^{ZZ} in the following form:

$$S_{HH}^{ZZ} = S_{cc}^{\zeta\zeta} \cdot \left(\frac{3}{2} \overline{\cos^2 \gamma_{jk}} - \frac{1}{2} \right) \cdot \left(\frac{3}{2} \cos^2 \theta_H - \frac{1}{2} + \frac{\eta}{2} \cdot \sin^2 \theta_H \cdot \cos^2 \Phi_H \right) \quad (5)$$

with $\eta = (S_{aa}^{\zeta\zeta} - S_{bb}^{\zeta\zeta})/S_{cc}^{\zeta\zeta}$ being an "asymmetry parameter" that characterizes the anisotropy of the fluctuations of the (long molecular) axis relative to the axes a and b of the director system; γ_{jk} – angle between ζ and $\boldsymbol{r}_{jk}$; Φ_H – azimuthal angle of the magnetic field orientation in the director frame.

As a general result for the second moment of a single smectic-C (S_C) domain with a certain normal direction $\boldsymbol{n}$ assuming that for sufficiently large magnetic fields $\boldsymbol{e}_H$, $\boldsymbol{n}$, and $\boldsymbol{d}$ are co-planar (and hence $\cos 2\,\Phi_H = -1$ for all θ one now obtains:

$$M_2 = \frac{1}{N} \cdot \sum_{j=1}^{N} \sum_{k \neq (j)} \left(-\frac{3\gamma^2 \hbar}{2 r_{jk}^3} \cdot K_{\zeta\zeta}^{ZZ} \cdot S_{cc}^{\zeta\zeta} \right)^2 \cdot \left\{ \left(\frac{3}{2} + \frac{\eta}{2} \right) \cos^2 \theta_H - \left(\frac{1}{2} + \frac{\eta}{2} \right) \right\}^2 \quad (6a)$$

or, with

$$M_2(0) = \frac{1}{N} \cdot \sum_{j=1}^{N} \sum_{k \neq (j)} \left(-\frac{3}{2} \frac{\gamma^2 \hbar}{r_{jk}^3} \cdot K_{\zeta\zeta}^{ZZ} \cdot S_{cc}^{\zeta\zeta} \right)^2$$

$$M_2 = M_2(0) \cdot \left\{ \left(\frac{3}{2} + \frac{\eta}{2} \right) \cdot \cos^2 \theta_H - \left(\frac{1}{2} + \frac{\eta}{2} \right) \right\}^2 \quad (6b)$$

with $M_2(0)$ being the second moment for a sample perfectly aligned with all long molecular axes (on the average) along the original magnetic field direction (maximum polarization).

The angular dependence of M_2 under rotation of the sample by an angle Φ in a magnetic field is described by (6) since $\cos\theta_H$ obeys the relation

$$\cos\theta_H = \cos\delta \cdot |\cos\theta| + \sin\delta \cdot |\sin\theta| \,. \quad (7)$$

(θ is the angle between layer normal $\boldsymbol{n}$ and magnetic field direction, cf. Figure 2.)

The relation between θ and Φ depends on the special model (see Sect. 2.2.2. and 2.2.3).

With $f(\varphi)$ being the distribution function for the azimuthal angles φ of the layer normals about the original direction $\boldsymbol{e}_Z$ of the magnetic field and $p(\vartheta)$ being the probability density for $\boldsymbol{n}$ making an angle ϑ with $\boldsymbol{e}_Z$ we obtain

$$\overline{m_2(\Phi)} = \frac{1}{2\pi} \cdot \int_0^{\pi} f(\varphi)\, \mathrm{d}\varphi \cdot \int_0^{\pi} p(\vartheta) \cdot \left[\left(\frac{3}{2} + \frac{\eta}{2} \right) \cos^2 \theta_H - \left(\frac{1}{2} + \frac{\eta}{2} \right) \right]^2 \cdot \sin\vartheta \, \mathrm{d}\vartheta \,. \quad (8)$$

This general expression for the second moment allows to regard different models for the layer ordering (characterized by specific distribution functions $p(\vartheta)$, $f(\varphi)$) as observed experimentally in dependence on the polarizing conditions. Two special models will be discussed in detail in Sect. 2.2.2. and 2.2.3.

Besides, the influence of the asymmetry parameter η on the spectral proton NMR lineshape will be studied in Sect. 2.2.2.

From now on we shall omit the horizontal bar in these expressions and denote by $m_2(\Phi)$ always the (accordingly) averaged quantity.

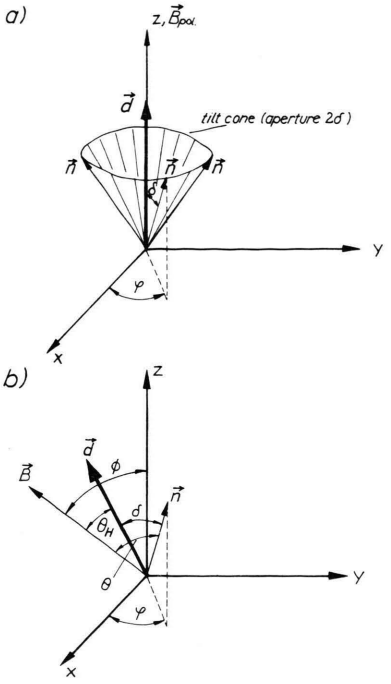

Fig. 2. Geometry of the smectic-C phase for maximum polarization in accordance with the model of Luz, Meiboom and Wise, Smith, Doane (LM/WSD). a) Initial state after polarization in the strong magnetic field $\boldsymbol{B}_{pol}$. b) After rotation of the magnetic field (or the sample, resp. to a new position (rotation angle φ).

2.2. Investigations on Oct-OAB and Hept-OAB

2.2.1. Experimental conditions

To align the samples studied here they were treated as follows: The samples were heated in a (measuring) magnetic field of (mostly) about 0.75 T into the isotropic phase. Then the field was switched to the corresponding polarizing field strength B_{pol} (for instance, 1.7 T), and after keeping the sample for some minutes in the isotropic phase at the field strength B_{pol} the temperature was lowered cautiously (especially at the phase transition) into the nematic phase. There the sample was kept for another 10 to 20 min before it was cooled down into the smectic-C state to the measuring temperature. In the vicinity of the nematic – smectic-C transition point the cooling rate was about 0.5 ... 1 K/min. After reaching the final temperature the magnetic field was set back to its former magnitude (generally about 0.75 T corresponding to a proton NMR measuring frequency of 32 MHz). The second moment data refer (for a certain substance) to one and the same temperature unless stated otherwise.

2.2.2. Maximum polarization – validity of the Luz-Meiboom/Wise-Smith-Doane model (LM/WSD)

To achieve maximum polarization (alignment) we applied the strongest magnetic polarization field B_{pol} (about 1.7 T) and very slow cooling rates. Inspite of the caution during the cooling process and equal maximum polarization fields the doublet peak splitting (and second moments) were not always maximum. Therefore the procedure has been repeated many times to get a "feeling" for the quality of the alignment. Only if the splittings (and second moments) were maximum and the spectra were well-structured (with distinct triplet shape, i.e., with a clear separation of central peak and outer doublet) the samples were used for studying the angular dependences. An additional aid to the judgement of the spectra with respect to overall sample alignment is provided by comparing them to the spectra of the corresponding nematic phases [17] that can easily be aligned.

Examples of the spectra of well-aligned samples of Hept-OAB and Oct-OAB are displayed in Figs. 8 and 9. Such well-polarized samples are characterized by a homogeneous alignment of the average direction of the long molecular axis d (from now often referred to as the molecular director) parallel to the external magnetic field direction. Assuming an average distance of the benzene of the protons of 2.45 Å an order parameter $S(= S_{zz}^{\zeta\zeta})$ of about 0.68 for Hept-OAB, and about 0.64 for Oct-OAB, resp., can be derived (neglecting the small angle between benzene ring para-axis and long molecular axis), still keeping in mind the uncertainties connected with the lack of the knowledge of the exact molecular geometry (cf. discussion in [17]).

The results of the computation are exhibited in Fig. 3 for tilt angles between 15° and 40°.

Comparing these curves with the experimental angular dependences of the second moments of Oct-OAB and Hept-OAB, resp., one would conclude to tilt angles of about 30° for Oct-OAB, and approximately 35° ... 40° for Hept-OAB. Thus we have plotted the experimental data together with the theoretical curves for tilt angles of 30° and 31.5° in Figure 4. (Oct-OAB), and for Hept-OAB with the theoretical dependences for tilt angles $\delta = 35°$, 36.5°, 37.5° in Figure 5. A fairly good fit can be obtained for tilt angles of 31.5° (Oct-OAB), and 37.5° (Hept-OAB), resp. The experimental $\overline{M_2(0)}$ represents the mean of the values of $M_2(0)$ and $M_2(180°)$. The "normalized" second moment $m_2(\Phi)$ is defined as

$$m_2(\Phi) = M_2(\Phi)/M_2(0) .$$

In both cases, the experimental data for two distinct temperatures are shown (in Fig. 4 below for

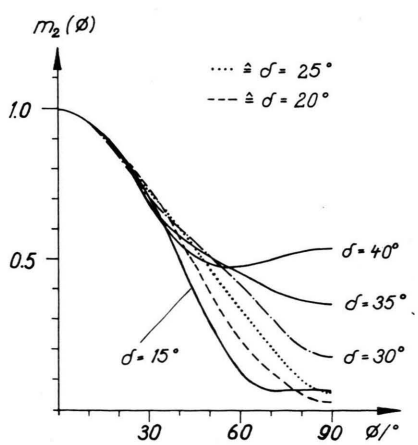

Fig. 3. Normalized second moment $m_2(\Phi)$ for maximum polarization as calculated after the LM/WSD model for several tilt angles δ.

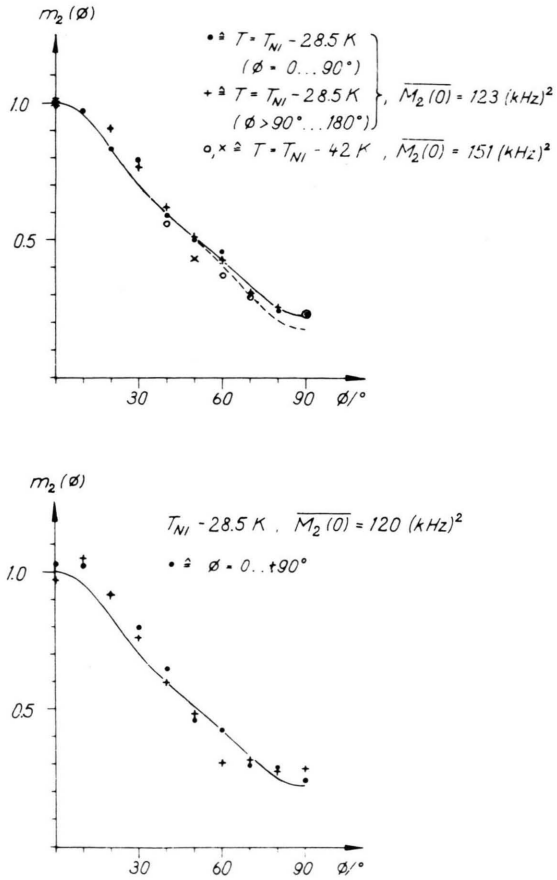

Fig. 4. Fit of the theoretical angular dependences $m_2(\Phi)$ to the experimental data for Oct-AB. Theoretical curves correspond to the LM/WSD model for tilt angles $\delta = 31.5°$ (——), and $\delta = 30°$ (- - -), resp., with $\eta = 0$.

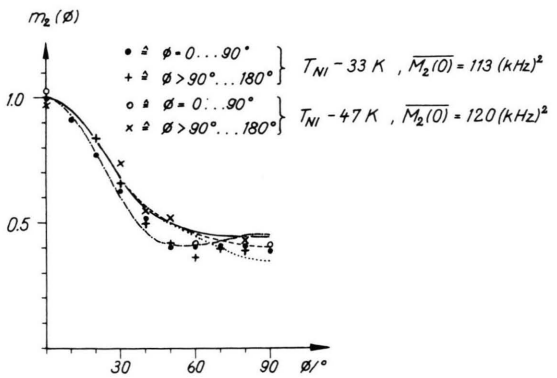

Fig. 5. The same as in Figure 4 for Hept-OAB. Theoretical curves are computed according to the LM/WSD model with $\eta = 0$ for $\delta = 37.5°$ (——). $\delta = 36.5°$ (- - -), and $\delta = 35°$ (· · ·), resp., as well as for $\delta = 40°$ with $\eta = 1$ (· — · — ·).

another measurement to document the reliability and reproducibility of the results). The good agreement of the data indicates the temperature independence of the tilt angle. (Generally the spectra for rotation angles between 0° and 180° were recorded. Since a symmetric behaviour of the second moment around $\varphi = 90°$ is expected and indeed observed and confirmed, the second moment values for angles greater 90° have been "mirrored" into the angular range between 0° and 90°. The different angular regions are marked by different symbols as explained in the figure captions.)

The influence of a finite value of the asymmetry parameter is depicted for tilt angles $\delta = 30°$ and 37.5° in Figure 6. Generally, positive η shifts the curves to lower $m_2(\Phi)$, negative η to greater ones. For noticeable deviations from the curve for $\eta = 0$, values of η greater than about 0.5 would be required. In general, however, one should keep in mind that asymmetric fluctuations of the long molecular axis in S_c phase could play a non-negligible role depending on the kind of experiment accomplished (e.g., ^{14}N nuclear quadrupole resonance [15], deuterium NMR [20]). In principle a fit to the experimental data is possible taking into consideration the asymmetry parameter (which has been determined by means of deuterium NMR by Photinos et al. [20] who observed a temperature dependent η growing with decreasing temperature from zero at the nematic – smectic-C transition up to about 0.5 ca 25 K below this transition for Hept-OAB) as demonstrated in Figure 6 for the case $\delta = 40°$, $\eta = 1$. However, we did not observe any temperature variation of the angular dependences within the range of our experimental accuracy.

Finally the influence of a distribution (of the polar angles) of the layer normals $p(\vartheta)$ shall be discussed. We have applied a very simple form for the distribution of the normals around the average direction (broadening or "smearing out" of the formerly sharp tilt cone), namely an equal distribution of angles ϑ between this average direction (by which the sharp tilt cone is defined, see Figure 2) and the actual normal direction within an interval of $\pm \Delta\sigma$. Obviously by this the value of the second moment M_2' at $\Phi = 0$ will be reduced compared to $M_2(0)$ of the perfectly aligned sample. In the following $M_2'(0)$ indicates that the value of M_2 at $\Phi = 0$ does *not* correspond to the maximum second moment of the totally aligned sample (simi-

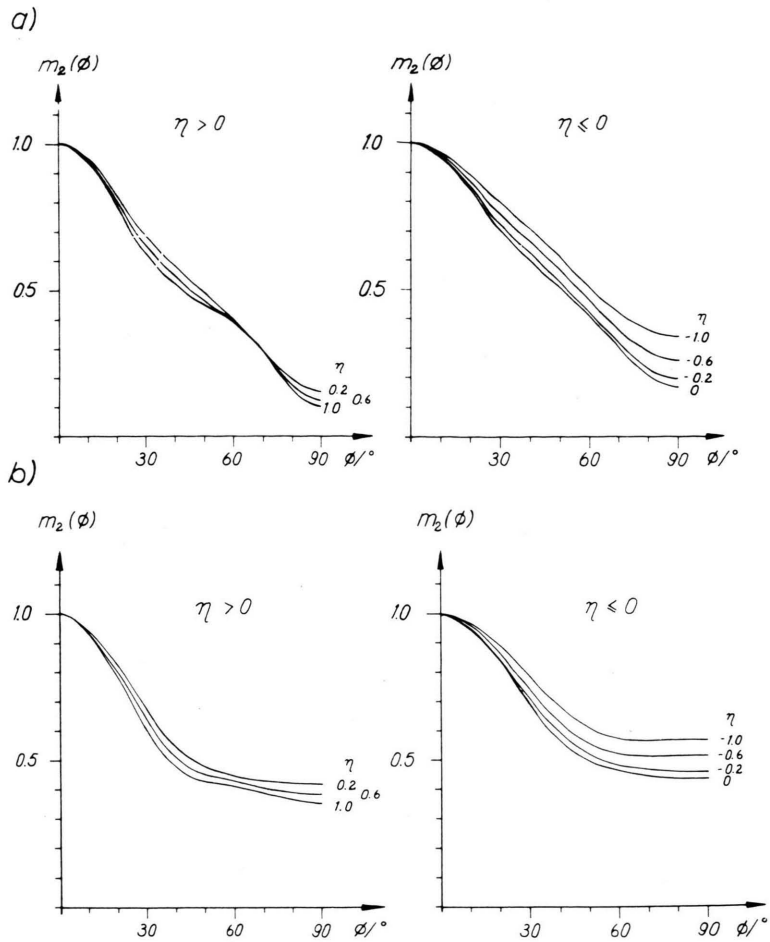

Fig. 6. Theoretical dependences $m_2(\Phi)$ accounting for asymmetry parameters η for a) $\delta = 30°$, and b) $\delta = 37.5°$.

larly, $m_2'(\Phi)$ denotes the ratio $M_2(\Phi)/M_2'(0)$, or $M_2(\Phi)/\overline{M_2'(0)}$, resp.). Thus a reduction factor R can be introduced by $M_2'(0) = R \cdot M_2(0)$.

In Fig. 7 the influence of different distribution widths $\Delta\sigma$ on the theoretical dependences $m_2'(\Phi) = M_2(\Phi)/M_2'(0)$ for tilt angles of 30° and 37.5° is demonstrated. General features are a flattening of the curves with increasing $\Delta\sigma$ and, of course, decreasing R (decreasing $M_2'(0)$). Even for fairly broad distributions (e.g., $\Delta\sigma = 40°$) the reduction is relatively moderate ($R \approx 0.62$ for $\delta = 30°$).

Using the before-mentioned (LM/WSD model we simulated the angular dependence of the proton NMR *lineshapes* in the smectic-C phases of Oct-OAB and Hept-OAB with tilt angles of 30° (Oct-OAB) and 37.5° (Hept-OAB), resp., starting from the spectra for $\Phi = 0$ which were computed by employing the procedure described and applied in [12, 14, 17] (cf. Figs. 8 and 9, resp.).

The agreement with the experimental dependences is obviously satisfactory, though the lineshape angular dependence seems to be less sensitive to details of the model than the second moment dependence (e.g. fairly little changes of the lineshape for angles $\Phi \gtrsim 60°$).

2.2.3 Imperfect alignment of the samples – dependence on the strength of the polarizing magnetic field

Here we shall discuss the effect of the magnetic field strength on the polarization of a smectic-C sample, i.e. the alignment of the molecular directors and the layer ordering. In their "classic" paper

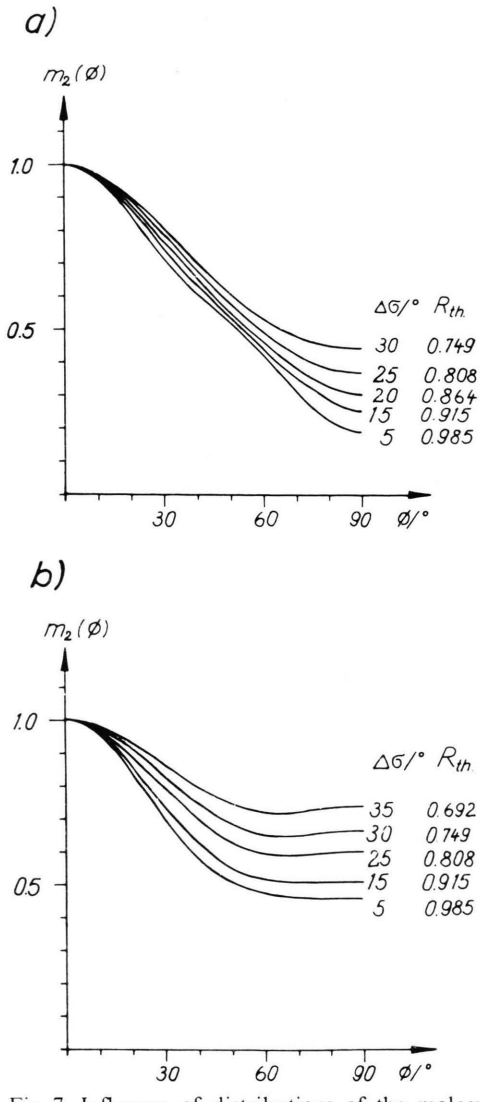

Fig. 7. Influence of distributions of the molecular directors $\boldsymbol{d}$ (width $\Delta\sigma$) about the direction of the initial (polarizing) magnetic field on $m_2(\Phi)$ for a) $\delta = 30°$, and b) $\delta = 37.5°$ (LM/WSD model). The theoretical reduction factor R_{th} is defined by $R_{th} = M_2'(0)/M_2(0)$ (see test for further details).

Wise et al. [9] reported already on an experiment in a weak magnetic field of about 0.15 T with observing the angular dependence of the spectra at the same field, whereas we only polarized the sample in weak fields, the spectra, however, were recorded mostly in measuring fields of about 0.75 T so that one can assume that the directors are able to reorient on the tilt cone to minimize the magnetic energy (cf. Section 2.2.2.). In weak magnetic fields

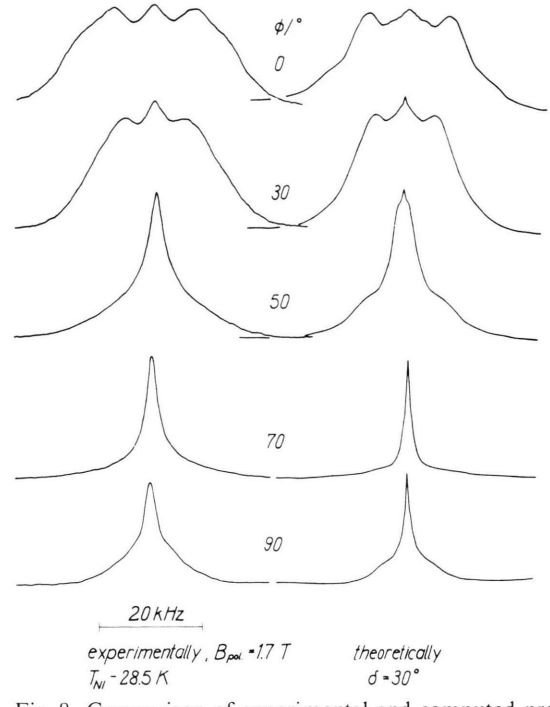

Fig. 8. Comparison of experimental and computed proton NMR spectra in dependence on the rotation angle Φ in the smectic-C phase of Oct-OAB ($\Delta\sigma = 0$, $\eta = 0$).

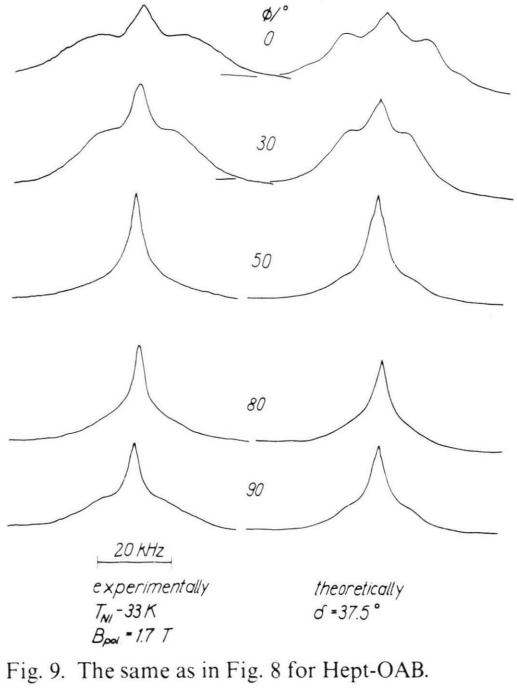

Fig. 9. The same as in Fig. 8 for Hept-OAB.

as in the experiment of Wise et al. [9] the field does not suffice to give rise to reorientations of the molecular directors on the tilt cone under rotation of the sample.

2.2.3.1. Oct-OAB and Non-OAB

A characteristic angular dependence $m_2'(\Phi)$ of a nonperfectly aligned S_c phase of Oct-OAB for a polarizing field strength of ≈ 0.75 T is shown in Fig. 10a: An essential feature of this plot consists in the fat that the maxima of both splittings and second moments appear at $\approx 30°$ and not at $\Phi = 0$ as expected in accordance with the LM/WSD model. This suggests that in the initial state of the polarized S_c phase at $\Phi = 0$ the molecular directors are not oriented pereferentially parallel to the magnetic field direction but are inclined at some angle of about 30° (i.e. approximately the tilt angle). Therefore the layers should be stacked preferentially perpendicular to the polarizing magnetic field direction or, expressed in another way, the layer normals are oriented preferentially parallel to the initial magnetic field direction thereby forcing the molecular directors $\boldsymbol{d}$ to make an angle δ with the magnetic field direction. Supposing again that the molecular directors are free to reorient about the layer normal direction $\boldsymbol{n}$ for the extreme case (with perfect alignment of all normals along the z-axis) the reduction factor should equal

$$[P_2(\cos\delta)/P_2(\cos 0)]^2 = [\tfrac{1}{2} \cdot (3\cos^2\delta - 1)]^2$$

(= 0.390625 for $\delta = 30°$; P_2 designates the Legendre polynomial of second order) and correspondingly the maximum of $m_2'(\Phi)$ (the relative superelevation of the curve) should amount to $[\frac{1}{2}(3\cos^2\delta - 1)]^{-2}$ and appear at $\Phi = \delta$. It seems conceivable that such a perfect stacking without any deviations is improbable. Therefore we admitted a layer normal distribution about the z-axis so that in a range of angles ϑ between 0 and $\Delta\sigma$ all normal orientations should be equally probable and outside this range no normal directions should occur. Certainly this represents only a fairly crude approximation, however, regarding the experimental (and theoretical) uncertainties, it should be sufficient.

In Fig. 10b the results of the computation of $m_2'(\Phi)$ for different distribution widths $\Delta\sigma$ are displayed. For the data represented in Fig. 10a a good fit of the theoretical curve can be attained with $\Delta\sigma = 20°$. The experimental reduction factor (for $M_2(0) \approx 120\,(\text{kHz})^2$, $M_2'(0) \approx 81\,(\text{kHz})^2$) $R_{\text{exp}} \approx 0.68$, however, is noticeably less than the theoretical one for $\delta = 30°$ (0.796). For this set of parameters ($\delta = 30°$, $\Delta\sigma = 20°$) we have simulated the lineshape angular dependence according to the model of PSL. The comparison of experimental (for $B_{\text{pol}} \approx 0.75$ T) and computed lineshapes is given in Figure 11. The agreement is obviously already fairly good. It could probably be improved yet by allowing for totally disordered regions in the sample (see discussion below).

Let us consider another model. If one regards the LM/WSD model as the limiting case describing the layer ordering under certain favourable conditions (see above), and the PSL model as the other extreme applying to low fields and/or unfavourable sample treatment then one could conjecture that at lower fields none of both models should be applicable in a "pure" form, but that rather a "mixing" or superposition of the two models should be present. That means, to a first approximation, one could try to match the data by ascribing a weighting factor p to, e.g., the portion behaving according to the LM/WSD model, whereas a fraction $(1-p)$ should obey the angular dependence demanded by the PSL picture (cf. Fig. 10a).

Another way to fit the data, assuming that the angular dependence can be described mainly by one of the models, would be to postulate the existence of a ordered fraction p' and a totally disordered one $(1-p')$ in the sample. "Ordered" here means that this fraction behaves as claimed by the model under consideration including in addition a layer distribution $\Delta\sigma$. The angular dependence is then described by

$$M_2(\Phi) = p'\, M_2^{\text{or}}(\Phi) + (1-p')\, M_2^{\text{do}} \qquad (15)$$

(M_2^{or} – second moment of the fraction obeying the angular dependence demanded by the model in question, M_2^{do} – second moment of the totally disordered sample). Note that in the smectic-C phase $M_2^{\text{do}} \neq \frac{1}{5} \cdot M_2(0)$ (see Section 2.2.2.). In the following calculations we have used the experimentally determined value of $M_2^{\text{do}} = 0.26 \cdot M_2(0)$ [16].

In Fig. 10c and d the experimental data for polarizing magnetic fields of 0.37 T and 0.165 T, resp., together with theoretical curves applying to the picture described above, are shown. Experi-

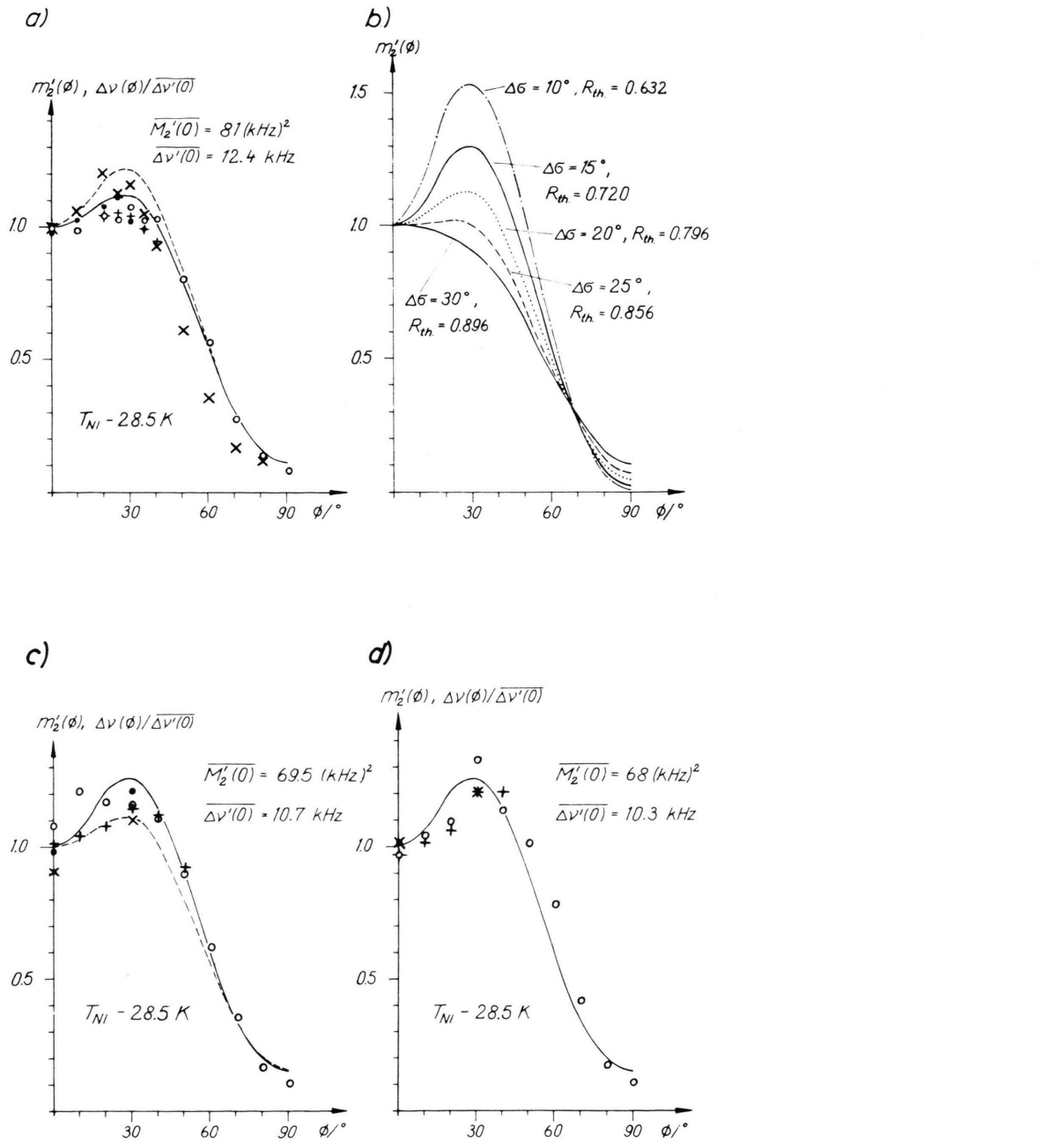

Fig. 10. a) Typical angular dependence of the normalized second moment $m_2'(\Phi)$ and splittings $\Delta\nu(\Phi)/\Delta\nu'(0)$ for a polarizing field of about 0.75 T in the smectic-C phase of Oct-OAB ($\circ \triangleq M_2$, $\Phi = 0 \ldots 90°$; $\times \triangleq M_2$, $\Phi > 90 \ldots 180°$; $+ \triangleq \Delta\nu$, $\Phi = 0 \ldots 90°$; $\bullet \triangleq \Delta\nu$, $\Phi > 90 \ldots 180°$). The solid line represents the theoretical curve according to the PSL model ($\delta = 30°$, $\Delta\sigma = 20°$) with disordered fraction ($p' = 0.8$, $R_{\text{theor}} = 0.689$), the dashed line is for the superposition of the LM/WSD model (with $\Delta\sigma = 35°$) and the PSL model ($\Delta\sigma = 15°$) with $p = 0.2$ and $\delta = 30°$ ($R_{\text{theor}} = 0.713$). b) Theoretical angular dependences $M_2'(\Phi)$ of the normalized second moment according to the PSL model with distribution $\Delta\sigma$ of the layer normals about the initial (polarizing) field direction. c) $B_{\text{pol}} = 0.37$ T (symbols as in a)). The solid line corresponds to the PSL model ($\Delta\sigma = 15°$) with disordered portion ($p' = 0.7$, $R_{\text{theor}} = 0.582$), the dashed one to the same picture with $\Delta\sigma = 20°$, $p' = 0.7$ ($R_{\text{theor}} = 0.635$), $\delta = 30°$ in both cases. d) $B_{\text{pol}} = 0.165$ T (symbols as in a). The solid line is for the PSL model with $\Delta\sigma = 15°$, $p' = 0.7$, $\delta = 30°$ ($R_{\text{theor}} = 0.582$).

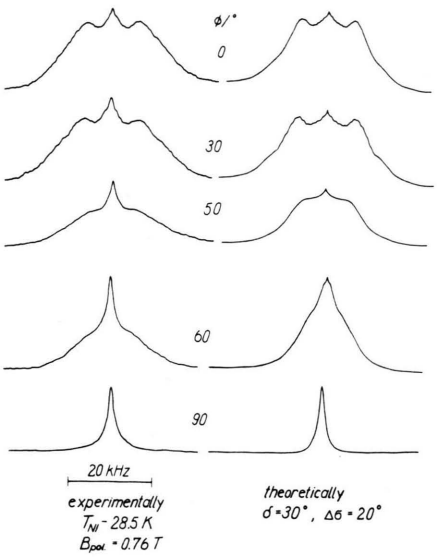

Fig. 11. Comparison of experimental and computed proton NMR lineshapes (PSL model with $\delta = 30°$ and $\Delta\sigma = 20°$) in the smectic-C phase of Oct-OAB.

mental reduction factors agree well with the theoretical ones employing the PSL model with disordered fraction (all relevant parameters are given in the figure captions).

Although the above-discussed mixing of the two models, or the superposition of ordered and disordered portions, resp., can be seriously questioned one has to realize that none of the pure models (even permitting wide distributions of the layer normal orientations $\Delta\sigma$) can explain simultaneously the angular dependences of the second moments for all polarizing fields *and* the decrease of $M_2'(0)$ (or, equivalently, R_{exp}) with decreasing B_{pol} in a satisfactory manner.

The dependence of the second moments at $\Phi = 0$ on the polarizing field is demonstrated in Fig. 12, where in *one* experiment (i.e. within about a few hours) the spectra at $\Phi = 0$ have been recorded for several polarizing fields between about 0.1 T and 1.7 T after the same polarizing treatment (as described in Sect. 2.2.1.). Data from measurements performed at other times are also indicated for comparison.

The decisive influence of the experimental conditions is documented in Figure 13. On slowly cooling down the sample from the nematic phase (especially at the phase transitions) the sample exhibits a good alignment (Fig. 13a). Its angular dependence can be described by the pure LM/WSD model with $\delta = 30°$ and $\Delta\sigma = 10°$. Even the reduction factor ($R_{theor} = 0.956$, $R_{exp} \approx 0.94$, assuming $M_2(0) = 120$ (kHz)^2) has about the correct value (keeping in mind the necessary caution in comparing the R's because of the big experimental errors).

If the sample, however, is cooled from the isotropic phase to the S_c phase at the natural cooling rate (i.e. on switching off the sample heating) quite a different angular dependence results as shown in Figure 14b. Evidently now the PSL model applies. The value of $\overline{M_2'(0)}$ (and R_{exp}) is much less than

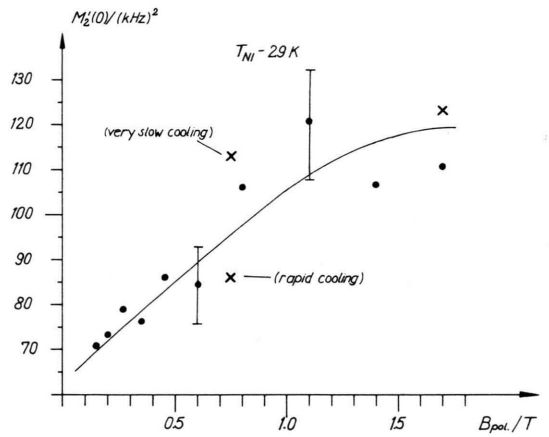

Fig. 12. Dependence of $M_2'(0)$ on the strength of the polarizing magnetic field B_{pol}.

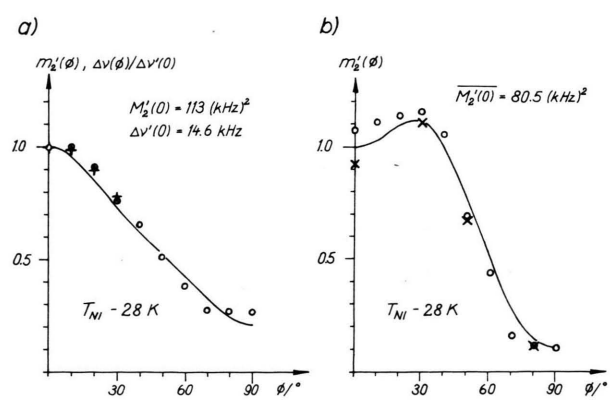

Fig. 13. Influence of the cooling rate on the quality of the alignment in presence of a polarizing field of ≈ 0.75 T. a) Very slow cooling rate (symbols have their former meanings as in Figure 10). The solid line represents the theoretical curve for the pure LM/WSD model ($\Delta\sigma = 10°$, $R_{theor} = 0.956$). b) Fast cooling (solid line corresponds to the PSL model with a disordered portion, $\Delta\sigma = 20°$, $p' = 0.8$, $R_{theor} = 0.689$). $\delta = 30°$ for both cases.

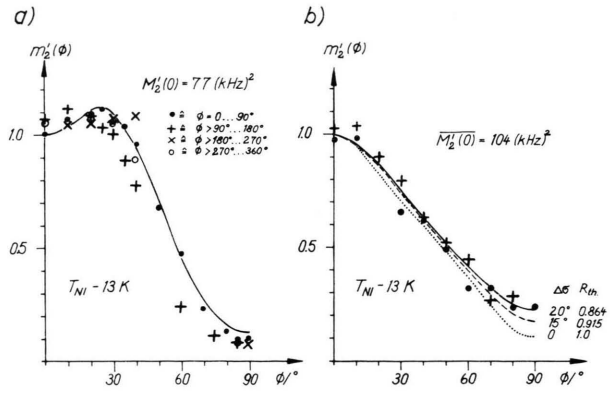

Fig. 14. Angular dependence $m_2'(\Phi)$ of the second moment in the smectic-C phase of Non-OAB at polarizing fields of a) 0.75 T. The solid line corresponds to the superposition of LM/WSD model ($\Delta\sigma = 35°$) and PSL model ($\Delta\sigma = 15°$) with $p = 0.3$ for $\delta = 27.5°$ ($R_{\text{theor}} = 0.752$); and b) about 1.7 T (maximum polarizing field), together with theoretical curves according to the LM/WSD model for different distribution widths $\Delta\sigma$. ● ≙ $\Phi = 0 \ldots 90°$; + ≙ $\Phi > 90° \ldots 180°$; × ≙ $\Phi > 180° \ldots 270°$; ○ ≙ $\Phi > 270° \ldots 360°$.

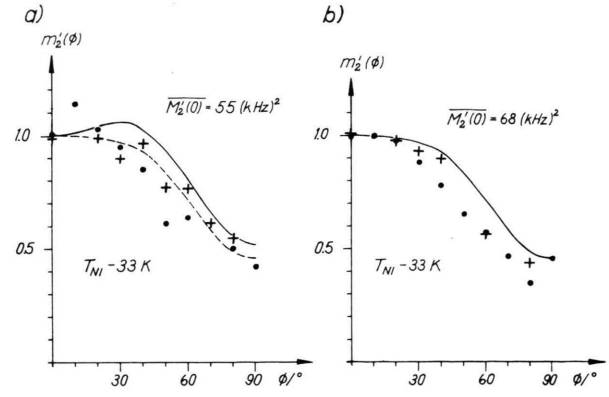

Fig. 15. Angular dependences $m_2'(\Phi)$ in the smectic-C phase of Hept-OAB for polarizing fields of a) 0.15 T. The solid line is for the PSL model ($\Delta\sigma = 30°$) with disordered fraction ($p' = 0.45$, $R_{\text{theor}} = 0.525$), the dashed curve for the same model with $\Delta\sigma = 35°$, $p' = 0.6$ ($R_{\text{theor}} = 0.627$); in both cases $\delta = 37.5°$; and b) 0.235 T. Solid line according to the PSL model with disordered portion ($\delta = 37.5°$, $\Delta\sigma = 35°$, $p' = 0.6$, $R_{\text{theor}} = 0.627$). ● ≙ $\Phi = 0 \ldots 90°$; + ≙ $\Phi > 90° \ldots 180°$).

before and a distinct elevation of the experimental plot at $\approx 30°$ is found. The data can be matched theoretically quite well under the same assumptions as in Figure 10a.

A similar angular dependence with an elevation of the $m_2'(\Phi)$ curve at some angle $\Phi \neq 0$ could be observed for Non-OAB, too (see Figure 14). A fit of the theoretical curves to the experimental is feasible supposing a PSL behaviour with $\delta = 27.5°$ and $\Delta\sigma = 15°$. The fit can still be improved assuming a mixing of the two models (see Figure 14). Of course, the same restrictions concerning the confidence of this procedure as discussed before still hold.

The best-aligned sample of Non-OAB (in a field of about 1.7 T) yielded an angular dependence as shown in Figure 14b. Again the experimental data can be interpreted in terms of the pure LM/WSD model with a tilt angle = 27.5° and layer distribution ($\Delta\sigma \approx 15° \ldots 20°$). Because of the uncertainties regarding the degree of the alignment a comparison of theoretical and experimental reduction factors appears not practicable.

2.2.3.2. Hept-OAB

In Fig. 15 two typical angular dependences of the second moments in the smectic-C phases of Hept-OAB are exhibited for polarizing fields of a) 0.15 T and b) 0.235 T together with the theoretical curves that yield the best fit (all appertaining prameters can be taken from the figure caption).

Again it is impossible to describe both the angular dependences and the reductions of the second moments $M_2'(0)$ (compared to the maximum value $M_2(0)$) equally well by any one of the "pure" models (with layer normal distribution alone).

Fitting curves can be achieved by assuming a disordered portion. Here we have to use the experimental value $M_2^{\text{do}} = 0.33\, M_2(0)$ [16].

It is somewhat astonishing that all angular dependences can be approximated theoretically by applying the PSL model whereas Leadbetter and Norris [1] did not observe such a behaviour for Hept-OAB (other than for Oct-OAB) in their X-ray investigations. However, for large distribution widths $\Delta\sigma$ (and, in some cases, small p'-values) the sharp differences between the two models should be effaced more or less (i.e. they should approach each other for large $\Delta\sigma$).

3. Summary

In this paper we present investigations on the behaviour of smectic-C phases possessing tempera-

Table 2. Tilt angles for the smectic-C phase of Hept-OAB as determined by different authors and methods.

X-ray	32 ± 2	[1]
X-ray	30	[2]
X-ray	38	[4]
X-ray	45	[19]
Optical/conoscopy	45	[5]
EPR	32.5	[6]
EPR	38.5 ± 1	[7]
NMR	45	[8]
NMR	45	[9]
Electric. conductance	33	[10]

ture independent tilt angles under rotation in magnetic fields of ≈ 0.75 T after previous alignment of the samples in fields of different strengths.

It could be shown that for the compounds studied here (which form smectic-C phases on cooling down from a preceding nematic phase without a smectic-A phase in between) it is rather difficult to get well-aligned samples, i.e. with all molecular directors initially being oriented perfectly parallel. Only on polarizing in strong fields ($\gtrsim 1.5$ T) and with slow cooling rates ones has good chances of obtaining well-aligned S_c-phases which can be reproduced.

From comparison of the angular dependences of such well-aligned samples with theoretical curves according to the wellknown Luz-Meiboom/Wise-Smith-Doane model [8, 9] tilt angles of about $37.5° \pm 2°$ (for Hept-OAB), and $30° \pm 2°$ (for Oct-OAB), resp., could be derived (for Non-OAB the estimation of the tilt angle of $27.5° \pm 3°$ is afflicted with some greater uncertainty because of very probably non-perfect polarization). The experimental data for lower polarizations were explained equally well using these tilt angle values which compare fairly well with the results of Leadbetter and Norris [1] for Oct-OAB ($30° \pm 2°$). For Hept-OAB they obtained a tilt angle of $32° \pm 2°$ whereas McMillan [4] (also by X-ray diffraction) determined a tilt angle of 38°. Former NMR investigations [8, 9] yielded a value of 45°. Generally, the range of experimentally measured tilt angles for Hept-OAB is fairly wide, which can be seen in Table 2. One important reason for this could consists in the varying quality of the overall sample alignment which is difficult to get even under the experimental conditions demanded before. Our values for the tilt angle seem to be intermediate.

4. Discussion

From the before-mentioned findings the *Question of the general validity of the LM/WSD model* arises even for well-aligned samples. Certain hints that it has to be modified in some ways are yielded by the determination of the ratio $f = M_2^{do}/M_2(0)$ that severely deviates from the values demanded by that model [16].

As to the occurrence of a layer arrangement with the normals being preferentially aligned along the polarizing magnetic field direction we are in accordance with Leadbetter and Norris [1] (for Oct-OAB) who from their X-ray diffraction results concluded the existence of such layer stacking especially if the samples were cooled from the nematic to the smectic state at the natural cooling rate.

At first sight such a behaviour seems to be incomprehensible. Taking into account, however, the fact that near the nematic – smectic-C transition still in the nematic phase smectic-C clusters are formed, (i.e., groups of molecules which show already a layer structure in small regions [1, 3, 4]), one could imagine that under certain circumstances (see above) the formation of a layer stacking as discussed in Sect. 2.2.3.1 is preferred over the parallel ordering of the molecular directors as it should normally be, especially in the case of S_c phases with a preceding smectic-A phase.

This picture is further supported by the observation of Chistyakov and Chaikovsky [3] that even in the nematic phases of the substances of this homologous series close to the S_c transition the molecules (which are contained in S_c clusters or "cybotactic groups") are not only inclined to the layer normals of the clusters but also to the direction of the polarizing magnetic field.

As pointed out already before, it is fairly easy to fit the experimental data without comparing the second moment at some given field to the maximum second moment, i.e., the task of allowing for both angular *and* field dependence of the second moment data is much more difficult. In the present paper we have proposed for this end some very simple and, admittedly, crude and somehow not quite satsifactory procedures as a zeroth approximation. If one, however, acknowledges that there are two extreme structures for the layer arrangement in the smectic-C phase it seems admissable to try if under inter-

mediate conditions the real behaviour can approximately be explained by a superposition of the two models (i.e. LM/WSD and PSL). Otherwise the assumption of disordered regions could be quite intelligible, too, if there is a non-perfectly polarized specimen. It has been demonstrated that this procedure works well for the description of the angular dependences of the proton NMR line shapes and second moments in smectic-A phases [18].

Acknowledgements

We are obliged to Prof. Dr. D. Demus, Dr. G. Pelzl, and Dr. S. Diele of the Halle liquid crystal group for placing at our disposal the substances studied here.

The authors gratefully acknowledge fruitful discussions and experimental support by Dr. H. Schmiedel and B. Hillner as well as useful talks with Prof. Dr. Lösche, Dr. K. Eidner and Dr. S. Grande.

[1] A. J. Leadbetter and E. K. Norris, Mol. Phys. **38,** 669 (1979).
[2] I. G. Chistyakov and W. M. Chaykovsky, Mol. Cryst. Liquid Cryst. **7,** 269 (1969).
[3] I. G. Chistyakov and W. M. Chaykovsky, Kristallografiya **18,** 293 (1973).
[4] W. L. McMillan, Phys. Rev. **A 8,** 328 (1973).
[5] T. R. Taylor, J. L. Fergason, and S. L. Arora, Phys. Rev. Lett. **24,** 359 (1970).
[6] E. Gelerinter and C. Flick, Chem. Phys. Lett. **44,** 300 (1976).
[7] G. R. Luckhurst, M. Ptak, and A. Sanson, J. Chem. Soc. Faraday Trans. II **69,** 1752 (1973).
[8] Z. Luz and S. Meiboom, J. Chem. Phys. **59,** 275 (1973).
[9] R. A. Wise, D. H. Smith, and J. W. Doane, Phys. Rev. **A 7,** 1366 (1973).
[10] G. Heppke and F. Schneider, Ber. Bunsen-Ges. Phys. Chem. **78,** 981 (1974).
[11] D Demus, H. Demus, and H. Zaschke, Flüssige Kristalle in Tabellen, Deutscher Verlag für Grundstoffindustrie, Leipzig 1974.
[12] H. Schmiedel, B. Hillner, S. Grande, A. Lösche, and St. Limmer, J. Mag. Res. **40,** 369 (1980).
[13] F. Volino and A. J. Dianoux, Mol. Cryst. Liquid Cryst.-Lett. **49,** 153 (1979).
[14] St. Limmer, H. Schmiedel, B. Hillner, and A. Lösche, and S. Grande, J. Physique **41,** 869 (1980).
[15] J. Seliger, R. Osredkar, V. Žagar, and R. Blinc, Phys. Rev. Lett. **38,** 411 (1977).
[16] St. Limmer, M. Findeisen, and H. Schmiedel, to be published.
[17] St. Limmer, M. Findeisen, H. Schmiedel, and B. Hillner, J. Physique **42,** 1665 (1981).
[18] A. Frieser, B. Hillner, and H. Schmiedel, Wiss. Z. KMU Leipzig (Math.-Natw. R.) **30,** 156 (1981).
[19] A. de Vries, Mol. Cryst. Liqu. Cryst. **10,** 31 (1970).
[20] D. J. Photinos, P. J. Bos, J. W. Doane, and M. E. Neubert, Phys. Rev. **A 20,** 2203 (1979).